

General Disclaimer

One or more of the Following Statements may affect this Document

- This document has been reproduced from the best copy furnished by the organizational source. It is being released in the interest of making available as much information as possible.
- This document may contain data, which exceeds the sheet parameters. It was furnished in this condition by the organizational source and is the best copy available.
- This document may contain tone-on-tone or color graphs, charts and/or pictures, which have been reproduced in black and white.
- This document is paginated as submitted by the original source.
- Portions of this document are not fully legible due to the historical nature of some of the material. However, it is the best reproduction available from the original submission.

NAG 3-341

Adsorption of O_2 , SO_2 , and SO_3 on Nickel Oxide.

Mechanism for Sulfate Formation

by

S. P. Mehandru[†]

and

Alfred B. Anderson

Chemistry Department, Case Western Reserve University

Cleveland, Ohio 44106



Abstract

Calculations based on the atom superposition and electron delocalization molecular orbital (ASED-MO) technique suggest that O_2 will adsorb preferentially end-on at an angle 45 deg from normal on a nickel cation site on the (100) surface of NiO . SO_2 adsorption is also stronger on the nickel site; SO_2 bonds through the sulfur atom in a plane perpendicular to the surface. Adsorption energies for SO_3 on the nickel and oxygen sites are comparable in the preferred orientation in which the SO_3 plane is parallel to the surface. The calculations suggest that the strength of adsorption varies as $O_2 > SO_2 > SO_3$. On activation, SO_3 adsorbed to an O^{2-} site forms a trigonal pyramidal SO_4 species which yields, with a low barrier, a tetrahedral sulfate anion. Subsequently the anion reorients on the surface. Possibilities for alternative mechanisms which require the formation of Ni^{3+} or O^{1-} are discussed. $NiSO_4$ thus formed leads to the corrosion of Ni at high temperatures in the $SO_2 + O_2 / SO_3$ atmospheres, as discussed in the experimental literature.

[†]On leave from KM College, Delhi University, Delhi 110007, India

85-32175

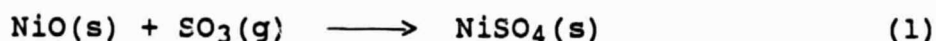
Unclas
21934

G3/26

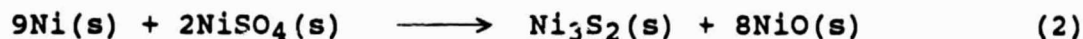
(NASA-CR-176072) ADSORPTION OF O_2 , SO_2 , AND
 SO_3 ON NICKEL OXIDE. MECHANISM FOR SULFATE
FORMATION (Case Western Reserve Univ.) 28 p
HC A03/NP A01 CSCI 11P

Introduction

The corrosion of nickel and nickel-based alloys in SO_2 and $\text{SO}_2+\text{O}_2/\text{SO}_3$ atmospheres has been investigated by several workers in the past.¹⁻⁹ Oxidation of nickel before it comes in contact with SO_2 gas results in the formation of an adherent protective scale of NiO on the nickel surface. This scale should, at first sight, prevent rapid corrosion of nickel in SO_2 atmospheres. Experimental results indicate that the corrosion rates of nickel in SO_2 atmospheres in the absence of O_2 at 600 °C are 10^4 to 10^6 times faster than its oxidation rate in 1 atmosphere oxygen.¹ This enormous difference has been attributed to the rapid transport of nickel through a continuous Ni_3S_2 phase in the NiO scale. It has been observed that the NiO scale cracks after an incubation period of 1 to 24 hours (depending upon the temperature and SO_2 pressure) presumably because of stresses generated by sulfide formation at the scale-nickel interface by molecular transport of SO_2 through the physical defects in the NiO scale.^{2,3} This may be followed by the rapid inward diffusion of SO_2 through the cracks to the metal surface resulting in rapid corrosion.² The corrosion behavior at 500-900 °C of preoxidized nickel in an $\text{SO}_2+\text{O}_2/\text{SO}_3$ environment, however, has been observed to be significantly different. Scale porosity is not a factor in the $\text{SO}_2+\text{O}_2/\text{SO}_3$ environment whereas it is definitely important in SO_2 atmospheres.³ This led previous workers to conclude that the initial reaction in the presence of SO_3 takes place on the NiO surface rather than at the nickel-nickel oxide interface. It is believed that nickel sulfate forms according to the reaction



NiSO_4 is thermodynamically stable only when the effective pressure of SO_3 in the gas mixture is higher than its equilibrium pressure in reaction (1). Rapid corrosion rates of nickel are observed when it is surrounded by a Pt catalyst^{1,3-5} which speeds the attainment of the $\text{SO}_2 + \frac{1}{2} \text{O}_2 \rightleftharpoons \text{SO}_3$ equilibrium. This shows the importance of SO_3 in the preliminary step of the overall corrosion reaction. The fact that NiSO_4 has been difficult to detect on the surface led to the conclusion that it must react rapidly with nickel which is diffusing outward through the NiO scale to form the sulfide phase according to the reaction^{1,4-7}



In fact, powdered mixtures of Ni and NiSO_4 have been found to react rapidly above 500 °C to form NiO and Ni_3S_2 .⁴ The rate of sulfide formation is, therefore, highly likely to depend on the rates of the proposed reaction steps (1) and (2).

In order to explain the mechanism of formation of the sulfide phase, it was tentatively assumed in Ref. 4 that the tendency for adsorption on the surface varies as $\text{SO}_3 > \text{SO}_2 > \text{O}_2$. Our results in this paper, however, suggest that the order is just the reverse. Therefore, the purpose of this paper is two-fold: firstly, to calculate the relative adsorption energies of O_2 , SO_2 , and SO_3 molecules on the NiO surface and to understand the binding of these species from the molecular orbital point of view; and, secondly, to calculate the potential energy surface and thus devise a reaction path for reaction (1). We use the atom superposition and electron delocalization molecular orbital (ASED-MO) theory which has been previously used in studying a number of sulfate formation mechanisms.¹⁰

Method of Calculation

The ASED-MO theory¹¹ is a semi-empirical technique based on an exact model in which the electronic charge density of a molecule or a solid is partitioned into a sum of rigid free atom components and a delocalization bond charge component. The superposition of rigid atom electron charge densities centered on the atomic nuclei yields, from the Hellmann-Feynman force theorem, a repulsive energy component, E_R . The attractive bond charge related energy component, E_D , is due to the interaction of a nucleus with the charge redistribution density according to the Hellmann-Feynman theorem. The sum is the exact molecular binding energy, E :

$$E = E_R + E_D \quad (3)$$

The E_D component of the total energy is not available but it has been found that the total molecular orbital energy, E_{MO} , obtained from diagonalizing a one-electron hamiltonian which shares some features of the extended Hückel hamiltonian is often a satisfactory approximation to E_D . We pay particular attention to ionization potentials¹² and Slater orbital exponents¹³ used in the determination of E_{MO} to produce accurate charge transfers and bond lengths for diatomic species. The parameters so determined are the basis for studying structures and reactions of larger systems. The parameters used in this paper are given in Table I.

Nickel oxide has the rock-salt structure. We have employed a two layer thick cluster containing 42 ions (21 nickel cations and 21 oxygen anions). The first layer consists of 9 Ni^{2+} and 12 O^{2-} ions, with the central Ni^{2+} ion surrounded by fully coordinated cations and anions in the same layer. This Ni^{2+} ion was used for

all adsorption studies on the Ni^{2+} site. The second layer has 12 Ni^{2+} and 9 O^{2-} ions, with central O^{2-} ion surrounded by fully coordinated cations and anions in the same layer. This O^{2-} ion was used for all adsorption studies involving the O^{2-} site. The two layers of the $\text{Ni}_{21}\text{O}_{21}$ cluster are shown in Fig. 1. There are 42 unpaired electrons in the cluster because each $d^8 \text{Ni}^{2+}$ cation has two unpaired electrons. This is consistent with allocating at least one electron to all the d band levels. For all our calculations, the heights of adsorbate molecules are optimized to the nearest 0.05 Å, the bond lengths to the nearest 0.01 Å, and the bond angles to 5 deg. The calculated O_2 bond length is 1.38 Å, somewhat overestimating 1.22 Å from experiment. The S-O bond lengths in SO_2 and SO_3 are 1.45 Å and 1.43 Å, respectively, compared to 1.43 Å from experiment for both. The calculated SO_2 bond angle is 119 deg compared to 119.5 deg from experiment.

Adsorption of O_2 , SO_2 , and SO_3 on NiO

We have calculated the structures and adsorption energies of O_2 , SO_2 , and SO_3 molecules on our nickel oxide cluster model (Fig. 1). For O_2 , both end-on (perpendicular and bent) and side-on (parallel) orientations on the central Ni^{2+} and O^{2-} ions of the cluster have been considered. The heights of O_2 above the surface site as well as the O-O bond length and tilt from the normal are completely optimized. Adsorption of SO_2 through the sulfur atom, as well as through the two oxygen atoms, is studied on the Ni^{2+} and O^{2-} sites. The SOO plane is kept perpendicular to the surface and the height, S-O bond lengths, and OSO angle are optimized. For SO_3 three orientations have been tried on the Ni^{2+} and the O^{2-} ions of

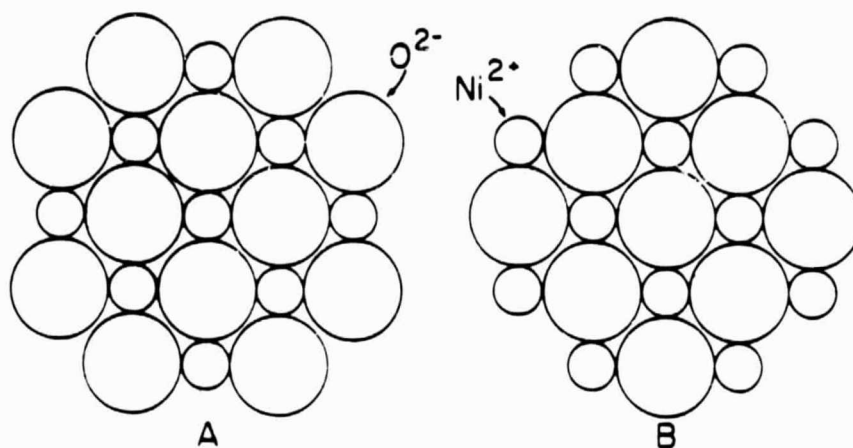


Fig. 1. A and B represent the two layers of the cluster model $Ni_{12}O_{21}$. For all adsorption studies on Ni^{2+} site, layer A is on the top and layer B on the bottom. For all adsorption studies involving O^{2-} site, layer B is on the top and layer A on the bottom.

the cluster. For the first orientation, binding is considered through the sulfur atom; the molecule is kept parallel to the surface and its height and the S-O bond lengths are optimized. In the second orientation SO_3 is constrained to bind to the surface Ni^{2+} and the O^{2-} ions through one of its oxygen atoms with the plane of the molecule perpendicular to the surface and then the height and the S-O bond lengths are completely optimized. In another orientation on O^{2-} , SO_3 is allowed to bind to the surface through its two oxygen atoms. All these orientations for O_2 , SO_2 , and SO_3 are illustrated in Fig. 2.

The calculated results for O_2 adsorption on the $\text{Ni}_{21}\text{O}_{21}$ cluster model are given in Table II. At first, perpendicular and parallel O_2 orientations are tried on the surface anion and cation sites. Of these, perpendicular coordination to Ni^{2+} is most favored. In this case the O_2 bond is found to stretch slightly by 0.06 \AA . Subsequent tilting produces additional stability, which is maximum at 45° from the surface normal. At this angle the O_2 bond stretches too much according to our non-self-consistent method, dissociating to produce oxide anions because the O 2p energy levels lie below the Ni valence band. In fact a charge self-consistent method would prevent this, but our result indicates that there is further weakening of the O_2 bond associated with the bending. When O_2 is coordinated parallel to a Ni^{2+} site, its bond shrinks by 0.05 \AA . Perpendicular and parallel O_2 orientations at the anion site produce less stability than the cation site. Tilting O_2 in the perpendicular orientation results in a slow and then rapid stabilization as it transfers to a neighboring Ni^{2+} site. The nature of the coordination bond between O_2 and Ni^{2+} may

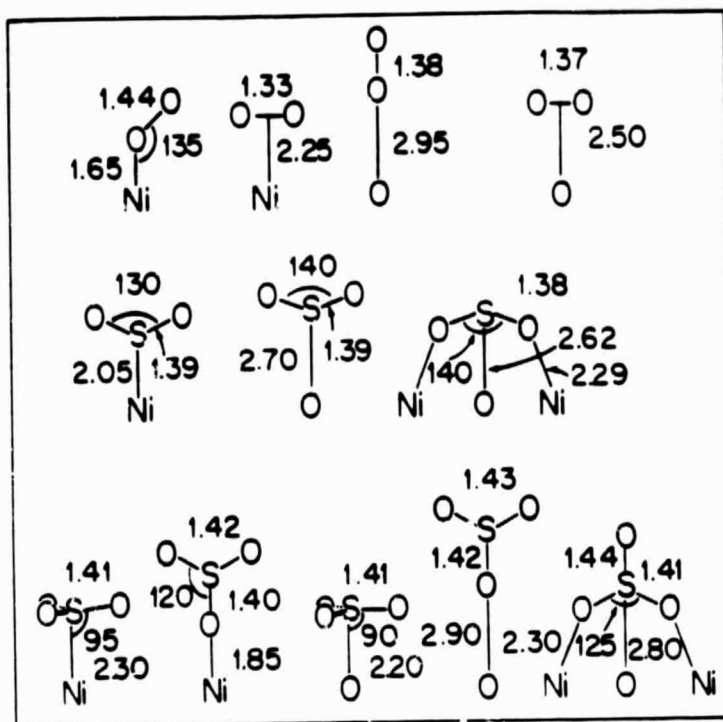


Fig. 2 Orientations of O₂, SO₂, and SO₃ studied on the Ni²⁺ and O²⁻ ions of the Ni₁₂O₂₁ cluster model. Only that surface ion is shown on which the adsorption is considered. Lengths are Å and angles are deg.

be understood from the energy level correlation diagram in Fig. 3. The first column of energy levels shows the valence levels of O_2 ; the second column shows how they shift as a result of the 0.06 \AA stretch; and the third shows the results of interacting with the cluster, for which levels are given in the fourth column. It may be seen that there is an important $O_2 \sigma_p$ donation bond to the $Ni^{2+} d_{z^2}$ orbital and that its antibonding counterpart lies high and, assuming the cluster spin does not change, it is empty. The O_2 orbitals form bonding and antibonding counterpart orbitals with what is formally labeled the O 2p band. There is no net bond order due to these interactions. It must be remembered that the O 2p band consists in $Ni^{2+} + O \text{ 2p}$ bonding orbitals which are predominantly O 2p in character but have some Ni d contributions. This is why the $O_2 \pi$ orbitals interact with the O 2p band when coordinated to Ni^{2+} . The $O_2 \pi^*$ orbitals form bonding orbitals with the Ni 3d band and they are doubly occupied. The antibonding counterpart orbital energy levels lie in the half-filled region, so there is a net back-donation to the $O_2 \pi^*$ orbitals which contributes to the adsorption bond order. The cause of the bending of O_2 away from the surface normal is evident in Fig. 3. With bending, the strength of the overlap between the π_x^* orbital and the d_{xz} orbital of Ni^{2+} decreases, resulting in reduced antibonding and, therefore, stability. As may be seen, two levels have dropped below the π_y^*, d_{yz} antibonding orbital levels; prior to bending they were degenerate. The resultant effect of all donation and back-donation interactions is a Mulliken charge transfer of 0.5 electron to the O_2 molecule, which weakens it and causes it to stretch. In

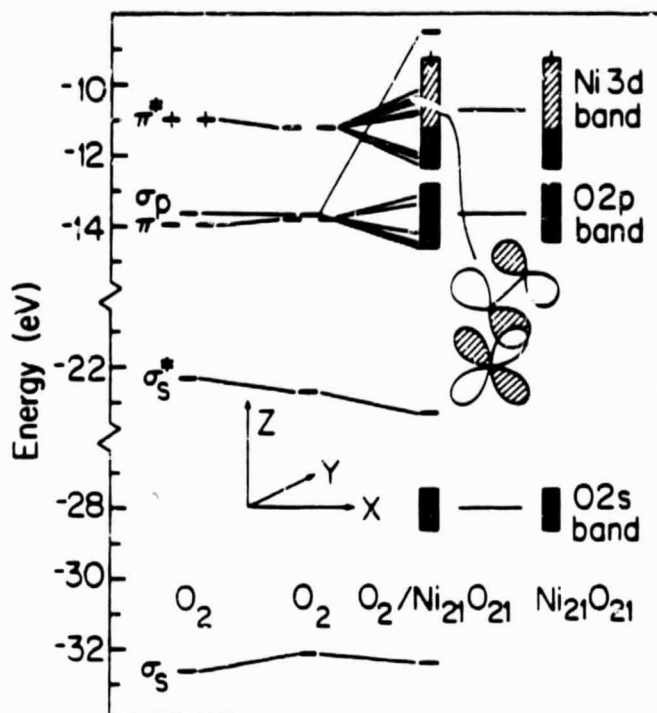


Fig. 3. Molecular orbital correlation diagram for O_2 adsorbed on the Ni^{2+} site in the end-on and bent orientation. The second column shows the energy levels of adsorbed O_2 without the surface. Correlation lines are drawn for orbitals which have 0.05 or more electronic charge on O_2 .

the parallel orientation the charge transfer is less, 0.1, and the O₂ bond shrinkage is probably a consequence of increased π -d bonding overlap and covalent stabilization.

The calculated structure and adsorption energy of SO₂ adsorbed through the sulfur atom on the Ni²⁺ and the O²⁻ sites of the cluster are tabulated in Table III. On adsorption the S-O bonds are shortened by 0.06 Å and the OSO angle increases by 10 deg on the Ni²⁺ site and 20 deg on the O²⁻ site, compared with the corresponding gas phase values. Adsorption is stronger on the Ni²⁺ site, as was the case for O₂. The orbital correlation diagram for SO₂ adsorbed on the Ni²⁺ ion is shown in Fig. 4. The second column shows the energy levels of SO₂ having the structure of the adsorbed molecule but with the surface removed. The lowest 2a₁ orbital of SO₂ is stabilized by a negative overlap, a phenomenon which has been seen in a variety of other studies as well,^{10c,14-16} and has been explained by Whangbo and Hoffmann using perturbation theory.¹⁵ This interaction yields a net stabilization because the antibonding counterpart lies high in the Ni 4p band, which is empty. The other significant interaction of SO₂ with NiO involves its 5a₁ orbital, the highest occupied orbital, with the d_{z²} orbital of Ni²⁺ ion, the antibonding combination of which is half-filled. This results in charge transfer from SO₂ to the Ni 3d band. There is however a weak back-donation to the 2b₁ orbital of SO₂, the lowest unoccupied orbital, to the d_{yz} orbital of Ni²⁺ ion. The net result is a transfer of about 0.3 electron from SO₂ to the nickel oxide. It is the reduction in occupation of the 5a₁ orbital which causes the OSO angle to increase by 10 deg, an expected result of molecular orbital theory.¹⁷ For this reason an increase in the OSO angle is

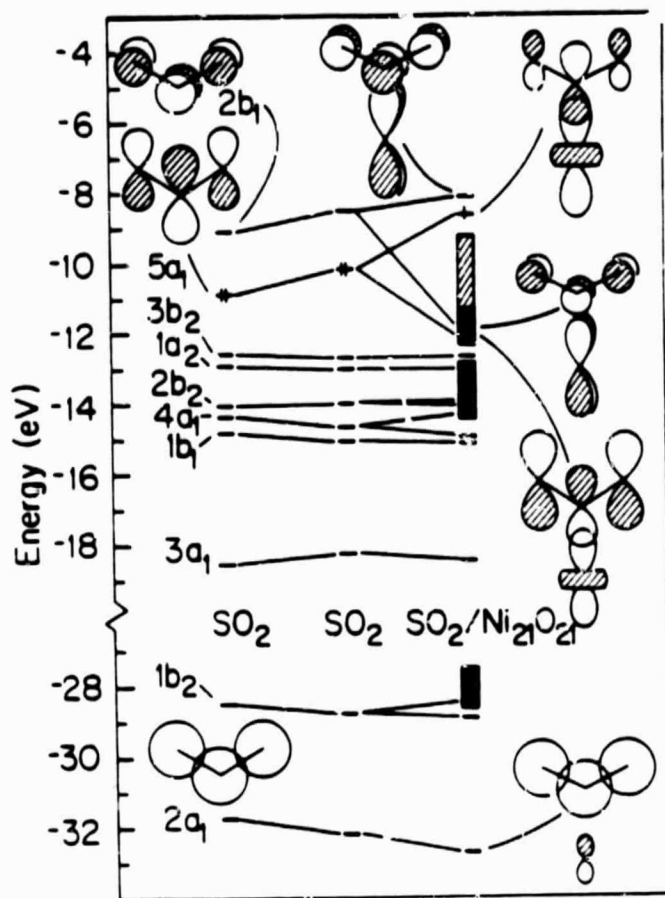


Fig. 4. Same as in Fig. 3 for SO_2 adsorbed through sulfur on the Ni^{2+} site with its plane perpendicular to the surface. The second column shows the energy levels of adsorbed SO_2 with the surface removed. Correlation lines are drawn for orbitals which have 0.2 or more electron on SO_2 .

also predicted for $\text{SO}_2\text{-O}^{2-}$ coordination and even for a mode of coordination where two oxygen atoms of SO_2 bond to two Ni^{2+} while bridging a central O^{2-} (Table III). Interestingly, in this last case, the $5a_1$ donation to the Ni^{2+} ions is through p_z orbitals on the oxygen atoms.

Table IV contains the calculated results for SO_3 adsorbed on the Ni^{2+} and the O^{2-} ions in all of the orientations described previously. As may be seen from this Table, adsorption energies for the parallel orientations far exceed those for the perpendicular orientations. Adsorption energies of SO_3 in the parallel orientation on the Ni^{2+} ion and the O^{2-} ion are within 0.2 eV of each other with Ni^{2+} site slightly favored. The S-O bonds are shortened by 0.02 Å and they bend upward by 5 deg when adsorbed on the Ni^{2+} site. The bending is caused in part by the small (0.01) negative Mulliken overlap between the oxygen atoms of SO_3 and the O^{2-} anions in the surface. The molecular orbital correlation diagram for SO_3 adsorbed on the Ni^{2+} site in the parallel orientation is shown in Fig. 5. The lowest orbital, $2a_1$, of SO_3 is stabilized by a negative overlap as discussed earlier for SO_2 . This interaction accounts almost entirely for the adsorption stabilization. The lowest empty orbital, $2a_2$, of SO_3 is stabilized by in-phase interaction with d_{z^2} of Ni^{2+} and this gives rise to charge transfer (-0.4) from the Ni 3d band to SO_3 . The corresponding antibonding counterparts lie high above and are empty. This orbital, being partially occupied, also contributes to the bending according to standard ideas of molecular orbital theory.¹⁷

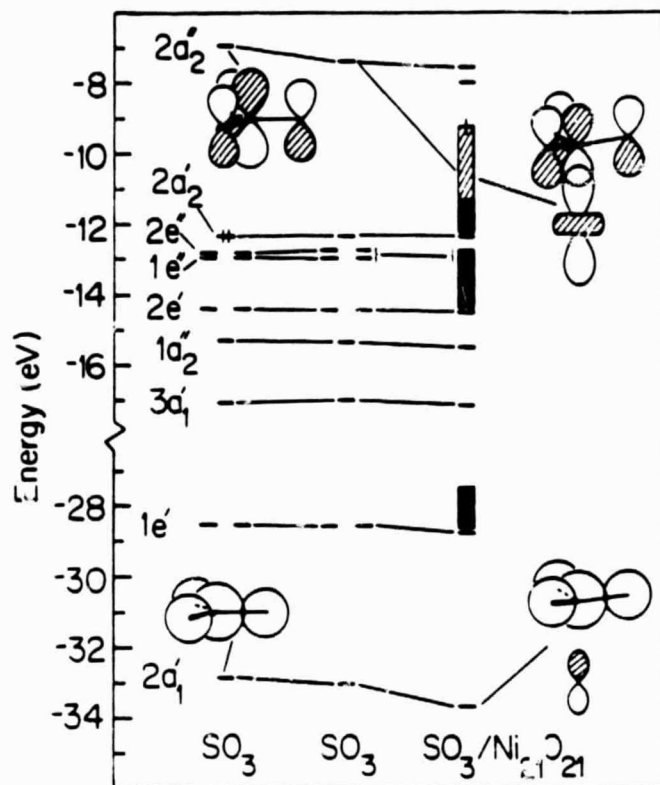


Fig. 5. Same as in Fig. 3 for SO₃ adsorbed in parallel orientation on the Ni²⁺ site. Correlation lines are drawn for orbitals with 0.2 or more electron on SO₃.

Mechanism of Sulfate Formation on Nickel Oxide in the Presence of O_2 , SO_2 , and SO_3

If we compare the calculated adsorption energies of O_2 , SO_2 , and SO_3 on the Ni^{2+} and the O^{2-} sites of the $Ni_{21}O_{21}$ cluster model, given in the previous section, the adsorption is favored on the nickel site for all the species. Thus if adsorption studies of each of these species on NiO are made at low temperatures and ultra high vacuum conditions, then they will adsorb on the Ni^{2+} ions of the oxide. However, if they are present at the same time at low temperatures and pressures, adsorption of O_2 on Ni^{2+} sites is preferred, thus blocking the nickel cations so that adsorption of SO_2 and SO_3 will be prevented. At high temperatures and pressures desorption will compete with adsorption and there is a likelihood of all species getting adsorbed and desorbed establishing a dynamical equilibrium between the condensed phase and the gaseous phase. Occasionally some SO_3 molecules will get adsorbed on the O^{2-} sites of the oxide surface forming a trigonal pyramidal SO_4 structure. We have calculated the reaction pathway for this trigonal pyramidal SO_4 species to convert to tetrahedral SO_4 . We calculate no activation barrier for the surface oxygen anion to come out of the surface plane accompanied by an umbrella distortion of S-O bonds, along with reorientation of SO_4 species until bonds are established between the two neighboring nickel cations and the lower two oxygens of SO_4 . The calculated structure of the coordinated sulfate is shown in Fig. 6. The calculated reaction energy of SO_3 and the $Ni_{21}O_{21}$ cluster model to give coordinated sulfate is 2.53 eV, about 1.1 eV more stable than the planar SO_3 adsorbed on the O^{2-} site of the cluster. The energetics for SO_4 formation from

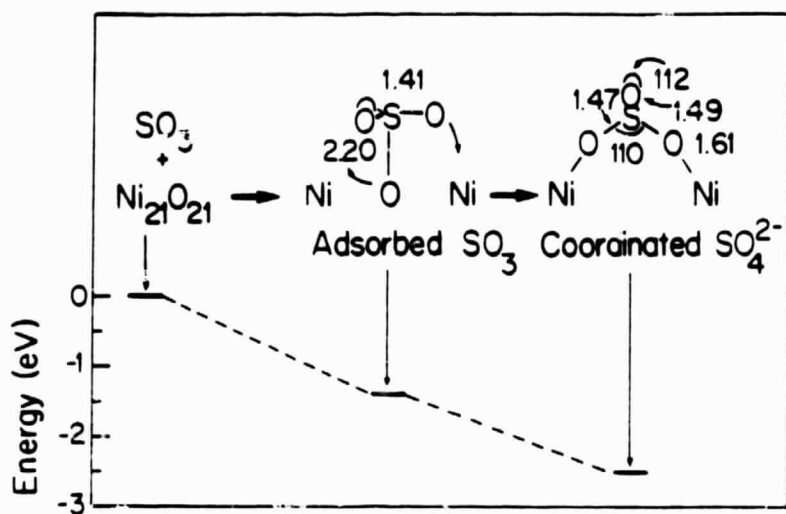


Fig. 6. Reaction pathway when adsorbed SO_3 on O^{2-} ion is converted to coordinated sulfate.

SO₃ and Ni₂₁O₂₁ cluster are also shown in Fig. 6. Our calculated reaction energy compares favorably with 2.61 eV calculated from the heats of formation values for the reactants and products of the reaction (1).¹⁸ Although our calculations produce no barrier for sulfate formation from SO₃ and Ni₂₁O₂₁, in practice, however, there may be a small barrier for displacing the O₂ molecules on the Ni²⁺ sites by SO₃ on the O²⁻ sites.

The orbital correlation diagram for SO₄²⁻ coordinated to Ni₂₁O₂₀²⁺ cluster is shown in Fig. 7. The lowest a-symmetry sulfate orbital is stabilized by negative overlap with the Ni P_z-orbitals. There are at least three other sulfate orbitals which show prominent in-phase stabilizations with the Ni s orbitals but their antibonding counterparts are also doubly occupied which makes these interactions closed-shell and non-bonding. However, the upper three filled orbitals of SO₄ are stabilized by mixing with Ni d orbitals and their antibonding combinations lie in the half-filled region of the Ni 3d band. This gives rise to charge transfer from SO₄²⁻ to the Ni 3d band. Our calculations produce a net charge of -0.3 on the coordinated SO₄ species.

At high O₂ pressures, alternate pathways to sulfate formation can be considered. It is commonly believed¹⁹ that Ni³⁺ and O¹⁻ form on the surface of NiO at high O₂ pressures. Therefore, under such conditions SO₃ may be expected to adsorb to O¹⁻ centers as well as O²⁻ centers, leading to the formation of sulfate. In the former case, as the sulfate anion forms, additional Ni³⁺ is created. Since Ni³⁺ is uncommon in solid nickel compounds it is relatively unstable and so may retard sulfate formation by SO₃.

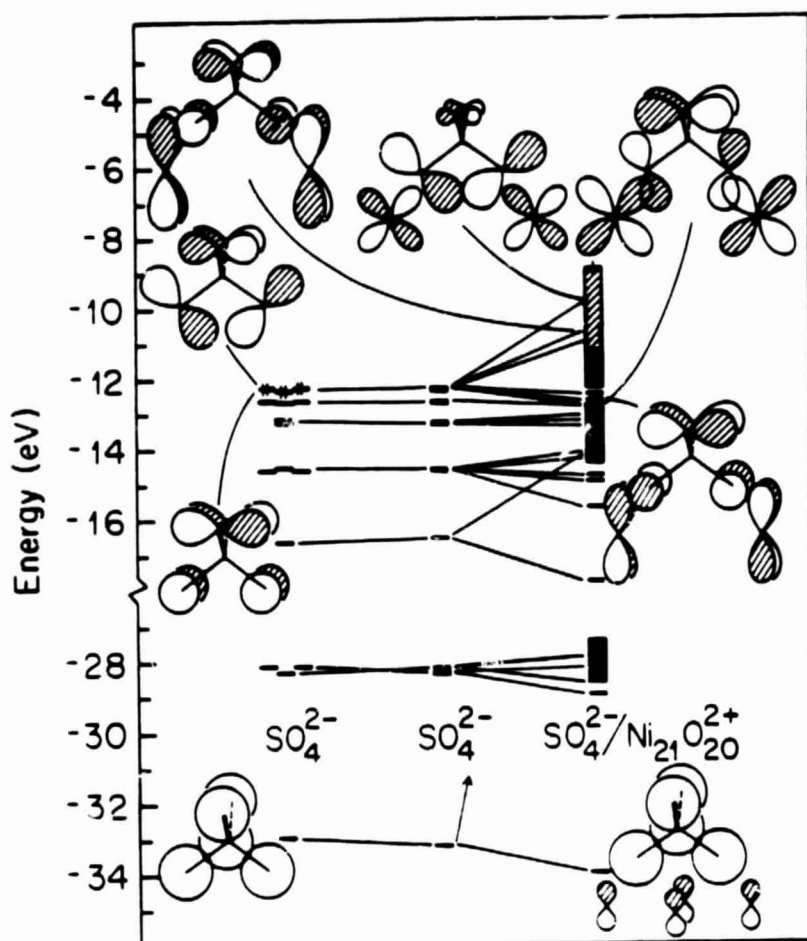


Fig. 7. Orbital correlation diagram showing SO_4^{2-} coordination to $\text{Ni}_{21}\text{O}_{20}^{2+}$ cluster. Correlation lines are drawn for orbitals with 0.2 or more electron on SO_4 .

attack on O^{1-} , should O^{1-} form on the surface. Another pathway might have SO_3 attack the upright activated adsorbed O_2 , just as in our past study of sulfate formation on a NaCl surface.^{10b} This reaction would lead to the formation of 3 Ni^{3+} or 3 O^{1-} whose relative instability may retard this pathway to sulfate formation. On the NaCl surface Cl^{1-} is oxidized to Cl_2 , a facile reaction. In the case of sulfate formation from SO_2 and a bis(phosphine) Pt dioxygen complex which we also studied theoretically,²⁰ the platinum is oxidized to Pt^{2+} , a facile reaction. The techniques of surface science (HREELS, UPS, XPS, and Auger) are appropriate for evaluating the importance of the above alternative mechanisms on NiO. We encourage that such studies of Ni^{3+} , O^{1-} and O_2 at the surface of NiO in the presence of O_2 be made.

Conclusions

Our study has characterized the binding of O_2 , SO_2 and SO_3 to the (100) surface of NiO. O_2 is predicted to bond the most strongly of the three molecules and SO_3 the least strongly. All bind more strongly to the Ni^{2+} cations than to the O^{2-} anions. The order of adsorption energies is probably not critical to the sulfate formation reaction, which involves O^{2-} donation to SO_3 to yield the SO_4 anion, because of the high gas pressures and temperatures of hot corrosion processes. According to our calculations, whenever SO_3 coordinates to a surface O^{2-} , sulfate is very likely to form because the calculated activation energy is low. We have not modeled the second step of the hot corrosion process, the reaction of nickel with the sulfate anion, in this study. However, it is known to proceed rapidly at high temperatures, just as does the

sulfate formation step. Finally, we encourage the surface science community to study the nickel oxide surface in the presence of O₂.

Acknowledgment

We thank the NASA Lewis Research Center for supporting this work through NASA Grant NAG-3-341.

References

1. a) K. L. Luthra and W. L. Worrell, *Met. Trans.*, 9A, 1055 (1978).
b) K. L. Luthra and W. L. Worrell, *Met. Trans.*, 10A, 621 (1979).
2. a) M. C. Pope and N. Birks, *Oxid. Metals*, 12, 173 (1978).
b) P. Kofstad and G. Akesson, *Oxid. Metals*, 13, 57 (1979).
3. W. L. Worrell and B. Ghosal, *Proc. Jap. Inst. Metals Suppl.*, 3, 419 (1983).
4. B. Heflan and P. Kofstad, *Corr. Sci.*, 23, 1333 (1983).
5. K. P. Lillerud, B. Haflan, and P. Kofstad, *Oxid. Metals*, 21, 119 (1984).
6. M. G. Hocking and V. Vasantasree, *Corr. Sci.*, 16, 279 (1976).
7. C. S. Giggins and F. S. Petit, *Oxid. Metals*, 14, 363 (1980).
8. V. Vasantasree and M. G. Hocking, *Corr. Sci.*, 16, 261 (1976).
9. C. B. Alcock, M. G. Hocking, and S. Zador, *Corr. Sci.*, 9, 111 (1969).
10. a) A. B. Anderson, *Chem. Phys. Letters*, 72, 514 (1980).
b) A. B. Anderson and N. C. Debnath, *J. Phys. Chem.*, 87, 1938 (1983).
c) A. B. Anderson and S. C. Hung, *J. Am. Chem. Soc.*, 105, 7541 (1984).
11. a) A. B. Anderson, *J. Chem. Phys.*, 60, 2477 (1974).
b) A. B. Anderson, *J. Chem. Phys.*, 62, 1187 (1975).
12. W. Lotz, *J. Opt. Soc. Am.*, 60, 206 (1970).

13. a) E. Clementi and D. L. Raimondi, J. Chem. Phys., 38, 2686 (1963).
b) H. Basch and H. B. Gray, Theoret. Chim. Acta, 4, 367 (1966).
14. A. B. Anderson, J. Catalysis, 67, 129 (1981).
15. M. H. Whangbo and R. Hoffmann, J. Chem. Phys., 68, 5498 (1978).
16. C. J. Marsden and L. S. Bartell, Inorg. Chem., 15, 2713 (1976).
17. See, for example, B. M. Gimarc, Molecular Structure and Bonding (Academic Press, New York, 1979).
18. Heats of formation for NiO(s), SO₃(g), and NiSO₄(s) are -58.4, -94.45, and -213.0 kcal/mole respectively. These values are taken from the Handbook of Chemistry and Physics, 43rd edition, C. D. Hodgman, Ed., The Chemical Rubber Publishing Co., Cleveland, Ohio, 1962.
19. N. Birks and G. H. Meier, Introduction to High Temperature Oxidation of Metals (Edward Arnold, London, 1983).
20. S. P. Mehandru and A. B. Anderson, Mechanism for Chelated Sulfate Formation from SO₂ and Bis(triphenylphosphine) Platinum, Inorg. Chem. 00, 0000 (1985).

Table I. Atomic parameters used in the calculations: Principal quantum number (n), ionization potential (IP) in eV, Slater exponents (ζ), and respective coefficients (c) for double- ζ d functions.

Atom	s		ζ	p		ζ	d					
	n	IP		n	IP		n	IP	ζ_1	c_1	ζ_2	c_2
Ni ^a	4	9.635	1.800	4	5.99	1.400	3	12.00	5.75	0.5681	2.00	0.6294
S ^b	3	22.200	2.220	3	12.36	1.927	3	6.00	1.90			
O ^{a,c}	2	27.480	2.046	2	12.62	2.027						

^aRef. 10a.

^bRef. 19.

^cFor the treatment of O₂, 3d orbitals with ionization potential 2 eV and Slater exponent 2.00, are also used (Ref. 10b).

Table II. Calculated results for the height (h), the change in O-O bond length after adsorption, $\Delta(\text{O-O})$, and the adsorption energy (ΔE) of O_2 on the $\text{Ni}_{21}\text{O}_{21}$ cluster model.

Site	Orientation ^a	$h(\text{\AA})$	$\Delta(\text{O-O})(\text{\AA})$	$\Delta E(\text{eV})$
Ni	End-on, 45 deg tilt	1.65	0.06	3.62
	Parallel	2.25	-0.05	2.71
O	Perpendicular	2.95	0.00	2.11
	Parallel	2.50	-0.01	2.39

^aSee Fig. 2.

Table III. Calculated results for the height (h) of the sulfur atom above the adsorption site, the change in S-O bond length, $\Delta(S-O)$, on adsorption, the OSO bond angle, and the adsorption energy (ΔE) of SO_2 adsorbed on the $Ni_{21}O_{21}$ cluster model.

Site	Orientation ^a	$h(\text{\AA})$	$\Delta(S-O)(\text{\AA})$	$\angle OSO(\text{Deg})$	$\Delta E(\text{eV})$
Ni	Perpendicular through sulfur	2.05	-0.06	130	2.66
O	Perpendicular through sulfur	2.70	-0.06	140	1.15
	Perpendicular through oxygens	2.62	-0.07	140	1.79

^aSee Fig. 2.

Table IV. Calculated results for the height (h) of the sulfur atom above the surface site, the S-O bond length (R_{SO}), and the adsorption energy (ΔE) of SO_3 when adsorbed on the $Ni_{21}O_{21}$ cluster model.

Site	Orientation ^a	$h(\text{\AA})$	$R_{SO}(\text{\AA})$	$\Delta E(\text{eV})$
Ni	Parallel through sulfur	2.30	1.41	1.59
	Perpendicular through one oxygen	3.25	(1.40, 1.42) ^b	0.62
O	Parallel through sulphur	2.20	1.41	1.41
	Perpendicular through one oxygen	4.32	(1.42, 1.43) ^b	0.06
	Perpendicular through two oxygens	2.80	(1.41, 1.44) ^c	0.68

^aSee Fig. 2

^bThe first number represents the bond length for one S-O bond perpendicular to the surface and the second number is the bond length for the other two S-O bonds of adsorbed SO_3 .

^cThe first number represents the bond lengths of the two S-O bonds through which SO_3 is binding to the surface and the second number is the bond length of the third S-O bond which is perpendicular to the surface.

Figure Captions

- Fig. 1. A and B represent the two layers of the cluster model $\text{Ni}_{21}\text{O}_{21}$. For all adsorption studies on Ni^{2+} site, layer A is on the top and layer B on the bottom. For all adsorption studies involving O^{2-} site, layer B is on the top and layer A on the bottom.
- Fig. 2. Orientations of O_2 , SO_2 , and SO_3 studied on the Ni^{2+} and O^{2-} ions of the $\text{Ni}_{21}\text{O}_{21}$ cluster model. Only that surface ion is shown on which the adsorption is considered. Lengths are Å and angles are deg.
- Fig. 3. Molecular orbital correlation diagram for O_2 adsorbed on the Ni^{2+} site in the end-on and bent orientation. The second column shows the energy levels of adsorbed O_2 without the surface. Correlation lines are drawn for orbitals which have 0.05 or more electronic charge on O_2 .
- Fig. 4. Same as in Fig. 3 for SO_2 adsorbed through sulfur on the Ni^{2+} site with its plane perpendicular to the surface. The second column shows the energy levels of adsorbed SO_2 with the surface removed. Correlation lines are drawn for orbitals which have 0.2 or more electron on SO_2 .
- Fig. 5. Same as in Fig. 3 for SO_3 adsorbed in parallel orientation on the Ni^{2+} site. Correlation lines are drawn for orbitals with 0.2 or more electron on SO_3 .

Fig. 6. Reaction pathway when adsorbed SO_3 on O^{2-} ion is converted to coordinated sulfate.

Fig. 7. Orbital correlation diagram showing SO_4^{2-} coordination to $\text{Ni}_{21}\text{O}_{20}^{2+}$ cluster. Correlation lines are drawn for orbitals with 0.2 or more electron on SO_4 .